

# Geophysical Research Letters<sup>®</sup>



## RESEARCH LETTER

10.1029/2022GL099299

### Key Points:

- Rising terrestrial water storage in Horn of Africa Drylands
- Increasing high-intensity rainfall events, particularly during October–November–December season
- Terrestrial water recharge correlates with seasonal high-intensity rainfall

### Supporting Information:

Supporting Information may be found in the online version of this article.

### Correspondence to:

M. Adloff,  
[markus.adloff@unibe.ch](mailto:markus.adloff@unibe.ch)

### Citation:

Adloff, M., Singer, M. B., MacLeod, D. A., Michaelides, K., Mehrnegar, N., Hansford, E., et al. (2022). Sustained water storage in Horn of Africa Drylands dominated by seasonal rainfall extremes. *Geophysical Research Letters*, 49, e2022GL099299. <https://doi.org/10.1029/2022GL099299>

Received 2 MAY 2022

Accepted 3 OCT 2022

### Author Contributions:

**Conceptualization:** Michael Bliss Singer, Katerina Michaelides, Chris Funk, Daniel Mitchell

**Funding acquisition:** Michael Bliss Singer, Katerina Michaelides, Daniel Mitchell







**Investigation:** Markus Adloff, Michael Bliss Singer, David A. MacLeod, Katerina Michaelides, Nooshin Mehrnegar, Eleanor Hansford

**Project Administration:** Michael Bliss Singer, Katerina Michaelides, Daniel Mitchell

**Supervision:** Michael Bliss Singer, Katerina Michaelides, Chris Funk, Daniel Mitchell

**Visualization:** Markus Adloff, Michael Bliss Singer, David A. MacLeod,

## Sustained Water Storage in Horn of Africa Drylands Dominated by Seasonal Rainfall Extremes

Markus Adloff<sup>1,2</sup> , Michael Bliss Singer<sup>3,4,5</sup> , David A. MacLeod<sup>1</sup> , Katerina Michaelides<sup>1,5,6</sup> , Nooshin Mehrnegar<sup>7</sup> , Eleanor Hansford<sup>1,8</sup>, Chris Funk<sup>9</sup>, and Daniel Mitchell<sup>1,6</sup> 

<sup>1</sup>School of Geographical Sciences, University of Bristol, Bristol, UK, <sup>2</sup>Now at University of Bern, Bern, Switzerland, <sup>3</sup>School of Earth and Environmental Sciences, Cardiff University, Cardiff, UK, <sup>4</sup>Water Research Institute, Cardiff University, Cardiff, UK, <sup>5</sup>Earth Research Institute, University of California, Santa Barbara, Santa Barbara, CA, USA, <sup>6</sup>Cabot Institute for the Environment, University of Bristol, Bristol, UK, <sup>7</sup>Department of Planning, Aalborg University, Aalborg, Denmark, <sup>8</sup>Now at European Centre for Medium-Range Weather Forecasts (ECMWF), Reading, UK, <sup>9</sup>Climate Hazards Center, University of California, Santa Barbara, Santa Barbara, CA, USA

**Abstract** Rural communities in the Horn of Africa Drylands (HADs) are increasingly vulnerable to multi-season droughts due to the strong dependence of livelihoods on seasonal rainfall. We analyzed multiple observational rainfall data sets for recent decadal trends in mean and extreme seasonal rainfall, as well as satellite-derived terrestrial water storage and soil moisture trends arising from two key rainfall seasons across various subregions of HAD. We show that, despite decreases in total March–April–May rainfall, total water storage in the HAD has increased. This trend correlates strongly with seasonal totals and especially with extreme rainfall in the two dominant HAD rainy seasons between 2003 and 2016. We further show that high-intensity October–November–December rainfall associated with positive Indian Ocean Dipole events lead to the largest seasonal increases in water storage that persist over multiple years. These findings suggest that developing groundwater resources in HAD could offset or mitigate the impacts of increasingly common droughts.

**Plain Language Summary** Over the last 40 years droughts are occurring more often in the Horn of Africa because of less rainfall during rainy seasons. We used satellite data to understand how rainfall has changed and how much water is stored on and below the land surface. We found that water storage is increasing, despite the poor rainy seasons. This is because heavy rain showers have become more common, which can most effectively refill the water stored in the ground.

## 1. Introduction

In the Horn of Africa Drylands (HADs), over 60% of the population lives with moderate or severe food insecurity, more than in any other region of the planet (FAO et al., 2019). Socioeconomic livelihoods in HAD are tied to highly variable seasonal rainfall, which has been inconsistent over recent decades (Lyon & DeWitt, 2012; Verdin et al., 2005; Wainwright et al., 2019; Williams & Funk, 2011). In this region, low rainfall in critical planting seasons creates major challenges for agro-pastoralist communities who depend on rainwater to grow crops, and on groundwater wells for drinking water. Over the last four decades, meteorological droughts in HAD have become more frequent and more severe (Funk, Shukla, et al., 2019; Liebmann et al., 2014; Lyon & DeWitt, 2012; Verdin et al., 2005; Williams & Funk, 2011). East Africa has been struck by 16 droughts since 2000, which generated severe food crises affecting millions of people (Funk, Thomas, et al., 2019). These droughts propagate into subsurface water storage (including soil moisture [SM] and groundwater stores), threatening regional food and water security in HAD (Dunning et al., 2018; Nicholson, 2017). During the 2016–2017 drought period, for example, more than 13 million people faced extreme hunger due to low crop yields (Funk et al., 2018), dryland areas faced extreme shortages of drinking water leading to disease outbreaks, and the livelihoods of millions of pastoralists were negatively impacted as millions of dollars' worth of livestock perished. Sequential October–November–December (OND) and March–April–May (MAM) droughts, typically associated with La Niña-like sea surface temperatures, can be particularly dangerous, as in 2010/2011, 2016/2017, 2020/2021, and 2021/2022. Since 2020 a similar, but even more severe five-season drought helped push 20 million Ethiopians, Kenyans and Somalians into severe insecurity in 2021 alone (FEWSNET, 2021), and poses an acute famine risk

© 2022. The Authors.

This is an open access article under the terms of the [Creative Commons Attribution License](https://creativecommons.org/licenses/by/4.0/), which permits use, distribution and reproduction in any medium, provided the original work is properly cited.

Katerina Michaelides, Nooshin Mehrnegar

**Writing – original draft:** Markus Adloff, Michael Bliss Singer

**Writing – review & editing:** Markus Adloff, Michael Bliss Singer, David A. MacLeod, Katerina Michaelides, Nooshin Mehrnegar, Eleanor Hansford, Chris Funk, Daniel Mitchell

across the region as we write. Given the precarious relationship between climate, the water cycle, and human lives and livelihoods in the HAD, there is a need to assess the sustainability of various components of the water balance over recent decades.

Over the last two decades in East Africa drylands, there have only been three MAM rainy seasons above the centennial average, while droughts occurred in nine out of the 20 years (Funk, Shukla, et al., 2019; Funk et al., 2018). This suggests that the “new normal” in HAD is characterized by lower-than-average MAM rainfall and rising drought frequency during a key growing season for HAD. Meanwhile, increasing rainfall in the OND season has been documented, with high interannual variability linked to the phase of the Indian Ocean Dipole (IOD; Liebmann et al., 2014; Nicholson, 2017), as well as to higher frequency of major flood events such as in 1997 and those that affected Somalia and Kenya in 2019 (FEWSNET Special Report, 2020). Despite documentation of these recent climatic changes, the impacts of MAM and OND rainfall on subsurface water storage across the HAD are currently unknown due to the lack of in situ observational networks for SM and groundwater. Remote sensing data have been used to estimate changes in parts of East Africa on local scales, over limited timeframes, or as part of global compilations (Bonsor et al., 2018; Kolusu et al., 2019; Shamsudduha & Taylor, 2020), but the broader picture of trends in spatial variability in water storage in response to seasonal rainfall across HAD is not known.

Drought propagation is poorly understood in drylands (Calow et al., 2010; MacAllister et al., 2020; Quichimbo et al., 2020). In dryland regions, hydrological partitioning of rainfall into infiltration, evapotranspiration, runoff, and groundwater recharge is highly sensitive to the spatial and temporal distribution of rainfall and most particularly, to the intensity and duration of individual rainfall events (Apuv et al., 2017; Cuthbert et al., 2019; Kipkemoi et al., 2021; Mileham et al., 2009; Singer & Michaelides, 2017; Taylor et al., 2013), rather than simply to total seasonal or annual rainfall. This is because the replenishment of groundwater (“recharge”) in drylands occurs mainly via focused recharge (transmission losses of flowing water into streambeds due to the predominance of surface runoff, Quichimbo et al., 2020) as well as by diffuse recharge (deep infiltration of water through soils). Sustained subsurface water storage in regions such as HAD therefore, depends on rainfall being of sufficient intensity to generate deep local infiltration and also surface runoff over the landscape that is routed to and recharged through porous ephemeral channels.

Trends in seasonal rainfall totals tend to be the focus of most HAD climate studies due to their importance for SM drought conditions during the primary MAM crop planting season (e.g., Agutu et al., 2017). Past work has revealed declining MAM and increasing OND rainfall (Harrison et al., 2019; Liebmann et al., 2014; Tierney et al., 2015), which might be expected to affect water storage. Here we explore the impacts of seasonal rainfall changes on water storage across HAD based on corroboration from multiple gridded data sets. Thus, we aim to address the causes and effects of water storage changes where there is a notable lack of in situ observational networks, and thereby make progress in understanding a consequential problem for the region. We (a) compare trends in seasonal rainfall within widely used rainfall data sets; (b) analyze decadal trends in Gravity Recovery and Climate Experiment (GRACE)-derived total water storage (TWS) and in shallow SM via the European Space Agency's Climate Change Initiative (ESA-CCI); (c) determine the dominant seasonal contributions to the TWS and SM signals via seasonal differencing; and (d) explore correlations between rainfall trends (in totals and extremes) and water storage trends across HAD. Our analysis is designed to generate new understanding of how HAD climate variability and trends have affected subsurface water storage in recent decades, and to address whether groundwater may potentially provide a robust resource for mitigating regional food and water insecurity.

## 2. Methods

Rain gauges with continuous records spanning multiple decades are rare and sparse in HAD. Assessments of rainfall anomalies and trends therefore often rely on gridded data based on: spatially interpolated rain gauges; a blend of point gauge data with remote sensing; reanalysis climate model data; or a combination of all these methods to assess corroboration between them: We selected six commonly used rainfall data sets representing this range of methods: GPCC, CRU, CHIRPS, ARC2, ERA5, and MSWEP (Text S1 and Table S1 in Supporting Information S1). We quantified multi-decadal trends in monthly and seasonal (MAM and OND) rainfall over the 1983–2016 period that is common to all data sets (Figure 1a), averaged over a  $1 \times 10^6$  km<sup>2</sup> area of HAD that exhibits bimodal rainfall in these seasons (black footprint in Figure 2a; Supporting Information S1; Nicholson, 2017). We took this multi-data set approach to identify consistent seasonal rainfall trends in HAD,

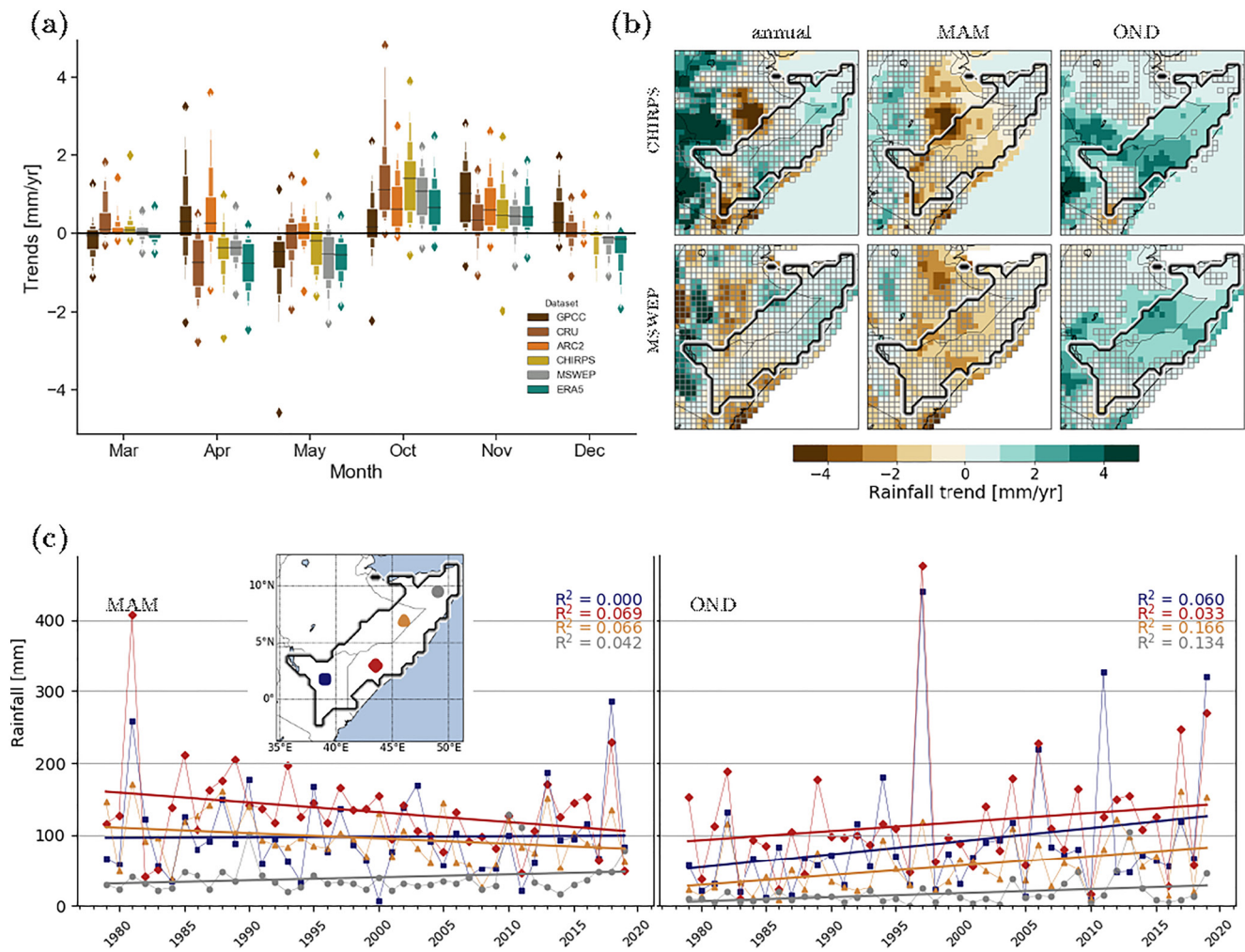


**Figure 1.** Rainfall trends over Horn of Africa Dryland (HAD). (a) Monthly rainfall trends within March–April–May (MAM; long rains) and October–November–December (OND; short rains) from six datasets. Each distribution represents the monthly rainfall trend across all pixels in the area framed black in panel (b). All trends are calculated over the period 1983–2016, depicted as the median and the 7th, 13th, 25th, 75th, 87th, and 93rd percentiles. Diamonds represent outliers. (b) Linearly approximated time series trends in annual, MAM and OND rainfall in HAD between 1981 and 2016. Grid cells with non-significant trends are framed in gray. (c) Time series of extreme seasonal rainfall total from MSWEP, 1979–2019 (falling in 3-hourly periods above the 95th percentile) in four equidistant locations across HAD, along with the approximated linear trend based on the Theil–Sen estimator (Supporting Information S1). The data for each location is averaged over an area of  $1.5^\circ \times 1.5^\circ$ .

because it has been shown that climate data sources have different strengths and weaknesses based on underlying methods and spatial and temporal resolutions. We then selected two widely used data sets with sub-monthly, CHIRPS (Funk, Peterson, et al., 2015), and sub-daily temporal resolution, MSWEP (Beck et al., 2019), to explore regional patterns of trends in seasonal and annual rainfall across HAD. The CHIRPS data set benefits from incorporation of a larger number of gauge observations in Ethiopia and Somalia, while the MSWEP gridded product has the advantages of high temporal resolution (3 hr) and incorporation of reanalysis climate data (Supporting Information S1).

In order to further understand the impact of rainfall on HAD water storage, we calculated trends in rainfall extremes (defined here as 3-hourly rainfall magnitude >95th percentile within MSWEP), and we compared these rainfall trends with secular trends in TWS from GRACE and in SM from the passive SM product of the ESA-CCI (integrated over an assumed depth of 10 cm, ESA-CCI 2021, [https://www.esa-soilmoisture-cci.org/sites/default/files/documents/public/CCI%20SM%20v06.1%20documentation/ESA\\_CCI\\_SM\\_D4.1\\_v2\\_PVIR\\_v6.1\\_issue\\_1.0.pdf](https://www.esa-soilmoisture-cci.org/sites/default/files/documents/public/CCI%20SM%20v06.1%20documentation/ESA_CCI_SM_D4.1_v2_PVIR_v6.1_issue_1.0.pdf); Section 2) for the years of overlap between these data sets (2003–2016).

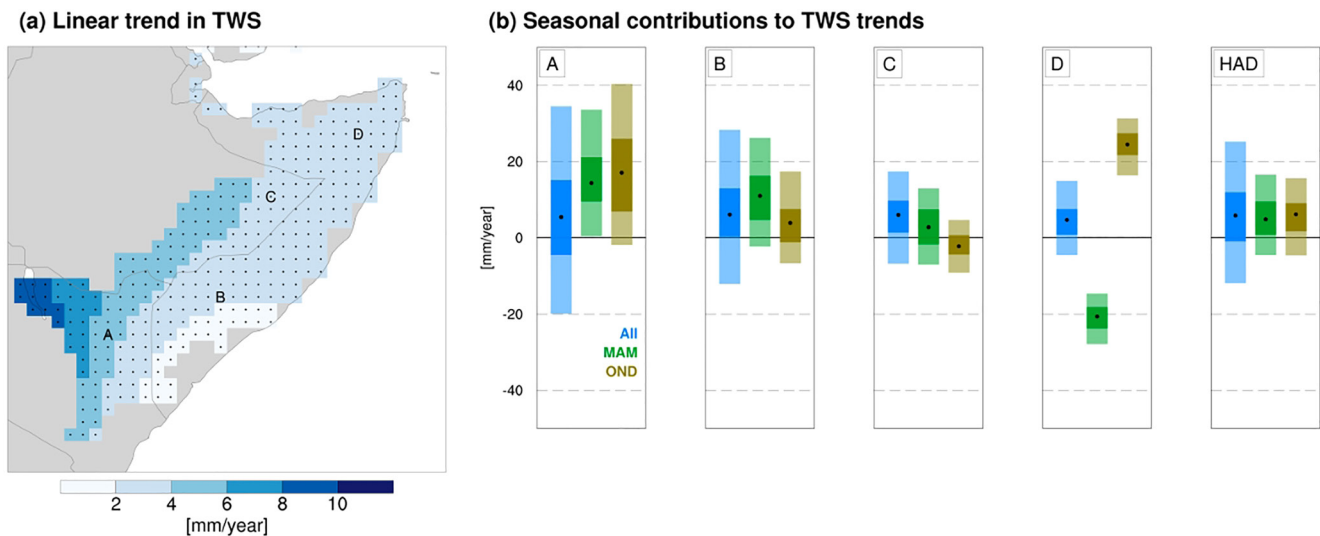


**Figure 2.** Horn of Africa Dryland (HAD) total water storage (TWS) trends. (a) Trends in monthly TWS over the period 2003–2016; stippling is applied at pixels where bootstrapping indicates the trend is not significantly different from zero. Irrespective of statistical significance (Amrhein et al., 2019), the average value of this trend across the HAD region is +4 mm/yr, which is consistent with that documented in Scanlon et al., 2022. (b) Bootstrapped overall trend and seasonal contributions to the TWS trend for the four locations indicated in panel (a) and for HAD as a whole. This subplot shows the overall linear trend in monthly TWS (All), and the contributions from long rains (March–April–May, MAM) and short rains (October–November–December, OND), based on accumulated  $\Delta$ TWS for each season (see “Creating  $\Delta$ TWS and  $\Delta$ SM” in Supporting Information S1); outer and inner box boundaries represent the 5th–95th and 25th–75th percentiles of the bootstrapped trend contribution estimates and the central dot indicates the median value.

For the correlation between TWS and SM with recharge with rainfall anomalies, we accounted for the initial state of TWS before each rainy season by computing TWS changes associated with MAM and OND seasons each year by quantifying the changes from the month before each season to the month after it, which we denote as  $\Delta$ TWS (Supporting Information S1). This method removes autocorrelation in the TWS signal and the overall TWS trend and ensures that we are computing TWS contributions arising only from seasonal rainfall by bracketing rainy seasons with typically dry periods. We assume that these dry-to-dry season differences will fully incorporate into the  $\Delta$ TWS signal the infiltrated rainfall and groundwater recharge occurring during a rainy season (Figure S5 and Text S1 in Supporting Information S1). Accordingly,  $\Delta$ TWS<sub>MAM</sub> was computed as  $TWS_{Jul} - TWS_{Feb}$ , and  $\Delta$ TWS<sub>OND</sub> was computed as  $TWS_{Feb} - TWS_{Sep}$ , and we used the accumulation of these increments to calculate trends in  $\Delta$ TWS associated with each rainy season over the GRACE period. We calculated seasonal SM changes by the same differencing method, denoted as  $\Delta$ SM. The choice of period of differencing enabled us to capture the change in dry-season values of TWS before and after MAM and OND rainy seasons.  $\Delta$ TWS<sub>OND</sub> for 2013 and  $\Delta$ TWS<sub>MAM</sub> for 2014 were not available because of data gaps in GRACE, so we linearly interpolated TWS for the missing months based on the TWS values of the previous and following months. We then estimated the extent to which  $\Delta$ TWS trends are associated with shallow SM versus deeper water storage (e.g., deep SM and groundwater).

Seasonal values and trends in total rainfall, rainfall extremes,  $\Delta$ TWS and  $\Delta$ SM were computed for all  $0.5^\circ$  pixels within the bimodal rainfall region (Figure 1c). To generalize these trends across the region, we spatially averaged over four roughly equidistant locations of  $3 \times 3$  pixels (22,500 km<sup>2</sup>) within HAD, located in Kenya, Ethiopia, Somalia and Somaliland (Figure 1c), based on the assumption that at an averaged scale of  $1^\circ$  and above, signal-to-noise ratios provide reasonable results for extreme rainfall (e.g., Roca, 2019). Our spatially averaged boxes of  $1.5^\circ \times 1.5^\circ$  thus allowed us to examine the impact of localized extreme precipitation, while not over-emphasizing local (single pixel) precipitation estimates. We also analyzed rainfall and water storage trends for all the pixels in this region.



### 3. Results

Our results show broad agreement between rainfall data sets, portraying negative MAM and positive OND rainfall trends over the period of analysis (Figure 1a and Figure S1 in Supporting Information S1). The consistency between data sets based on different methodologies, including a reanalysis product that does not include rain gauge data in HAD (ERA5), suggests that these trends are not an artefact of progressively decreasing numbers of rain gauges for the region, as has been suggested (Lorenz & Kunstmann, 2012; Maidment et al., 2015). The negative MAM trend is mostly due to total rainfall reductions in April and May, consistent with the documented trend of an earlier cessation of the long rains (Wainwright et al., 2019), while the positive OND trend is associated with higher rainfall in October and November (Figure 1a).

Our four selected locations across HAD exhibit both positive and negative trends in extreme MAM rainfall, but only positive trends in rainfall extremes for the OND season (Figure 1c and Figures S2 and S3 in Supporting Information S1). Averaged over HAD, seasonal rainfall totals decreased in MSWEP by approximately  $-0.9$  mm/yr (range across rainfall data sets:  $-1.6$  to  $-0.5$  mm/yr) since 1981 while OND rainfall increased by  $1.14$  mm/yr ( $0.0$  to  $1.8$  mm/yr) over the same period in MSWEP. MSWEP has the sufficient temporal resolution to identify high intensity rainfall events, and shows that these changes are largely due to changes in extreme rainfall, where rainfall above the 95th intensity percentile declined by  $-0.75$  mm/yr in MAM, while it increased by  $0.94$  mm/yr during OND. Additionally, in the last two decades HAD received on average as much rainfall during OND ( $123 \pm 109$  mm) as during MAM ( $124 \pm 49$  mm), despite the fact that OND has historically lower seasonal rainfall totals. Furthermore, the trends in extreme rainfall over this period are larger than trends in non-extreme seasonal rainfall, highlighting that recently a larger proportion of seasonal rainfall is occurring during extreme events than in the 1980s for both rainy seasons (Figures S3c and S3d in Supporting Information S1).

Over the GRACE period (2003–2016), we found that TWS exhibits a positive trend of  $\sim 4$  mm/yr (Figure 2a, Figure S6 and Table S2 in Supporting Information S1), suggesting that despite the increasing frequency of droughts and failing MAM rains (Figure 1; Funk, 2012), subsurface water storage has not declined, and is in fact rising across HAD. This rise in TWS based on contributions from both rainy seasons is most evident in inland areas of Kenya and in Ethiopia within the study area and less apparent over the southern coastal area of Somalia (Figure 2b). The short record and high interannual variability precludes statistical significance of these rising TWS trends (Supporting Information S1; Figure S7 in Supporting Information S1, Amrhein et al., 2019). Nevertheless, a bootstrapping analysis ruled out any significant negative trend in TWS (Supporting Information S1), and we suspect statistically significant positive TWS trends will develop in the future. For northern Kenya and southern Somalia (locations A and B), we find that the annual TWS storage trends are comprised of positive  $\Delta TWS$  from both seasons, while for Somaliland (location D), negative  $\Delta TWS_{MAM}$  is offset by strongly positive  $\Delta TWS_{OND}$ , producing an overall positive annual trend in TWS (Figure 2b). In contrast, positive  $\Delta TWS_{MAM}$  compensates for small negative  $\Delta TWS_{OND}$  in eastern Ethiopia (location C), leading to an overall positive trend in annual TWS (Figure 2b).

By investigating the pixel-by-pixel correlations between seasonal GRACE  $\Delta TWS$  trends (Figure 2b) and seasonal rainfall trends derived from MSWEP across the HAD region (Figure 3; see Figure S7 in Supporting Information S1 for the same analysis with CHIRPS), we find that  $\Delta TWS$  is positively correlated ( $r > 0.5$ ) with rainfall in both rainy seasons across most of HAD. However, there is high spatial heterogeneity and correlations are generally stronger in the southwest of HAD than in the northeast (Figure 3c), where the signal-to-noise ratio in rainfall estimates is high due to the higher aridity and lower seasonal totals. Across HAD, the correlation between  $\Delta TWS_{MAM}$  and MAM rainfall anomalies is slightly higher on average than between  $\Delta TWS_{OND}$  and OND rainfall, but the OND correlations are more spatially coherent. Annual values of  $\Delta TWS_{OND}$  and OND rainfall reveal the coincidence of positive IOD events (2006, 2011, and 2015), with high rainfall across HAD and large positive  $\Delta TWS$ . In these positive phase IOD years, most of the four locations in Figure 2a received above average amounts of extreme rainfall (Figure 1c), suggesting the importance of these rainfall extremes in supporting sustained water storage.

We further ascertained how much of the  $\Delta TWS$  variability can be explained by extreme rainfall by comparing the partial correlations between  $\Delta TWS$  and total rainfall separately from extreme rainfall ( $>95$ th percentile). Even though on average the extreme part of the distribution contributes to around half of the seasonal total rainfall, we found that these extremes explain a disproportionate amount of the variance in  $\Delta TWS$ . Specifically, rainfall

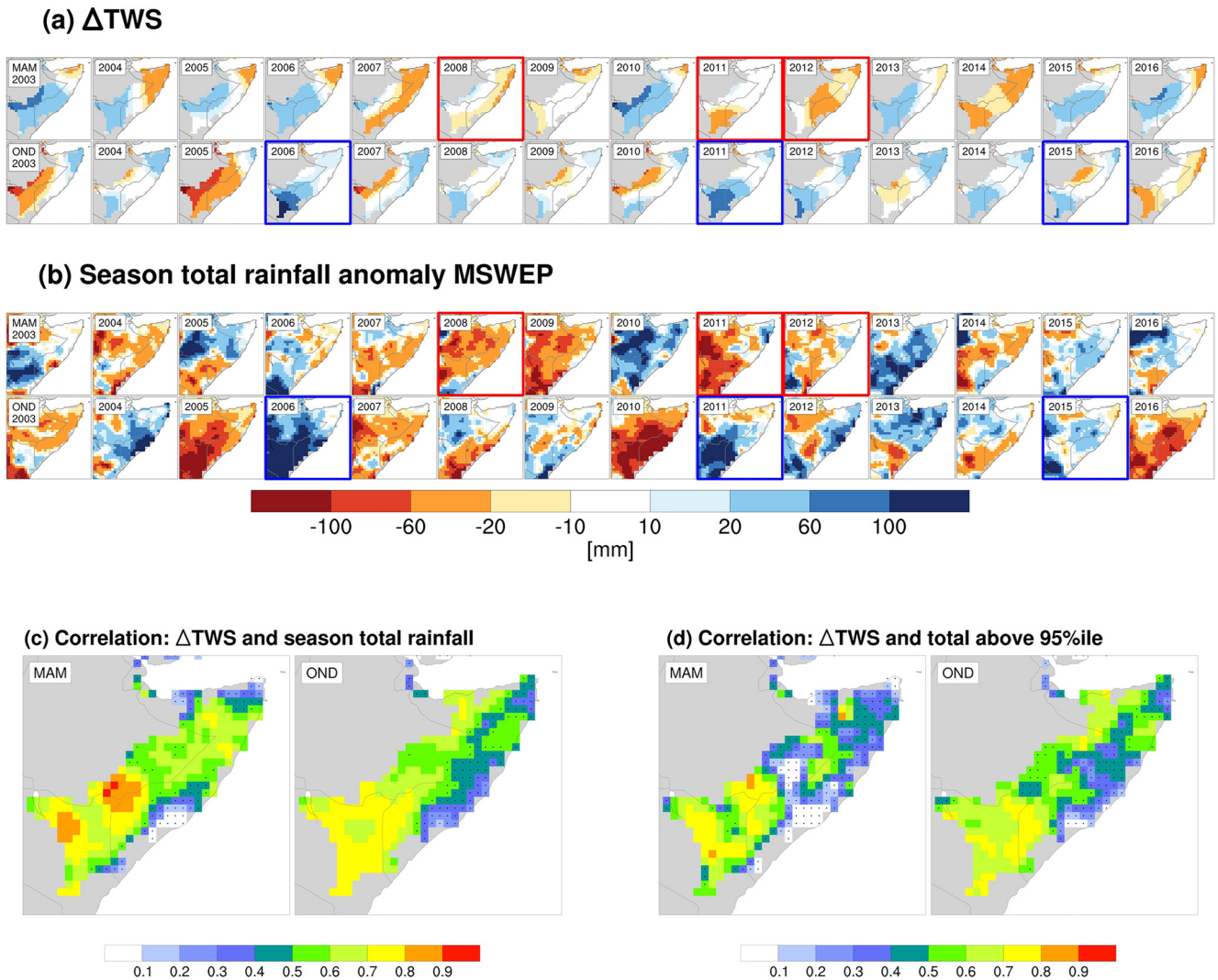


**Figure 3.** Correlation between groundwater and rainfall anomalies in Horn of Africa Dryland. (a) Annual values of  $\Delta TWS_{MAM}$  (top row) and  $\Delta TWS_{OND}$  (bottom row) over the period 2003–2016, within the masked area from Figure 1b. (b) MSWEP seasonal totals for March–April–May (MAM; top row) and October–November–December (OND; bottom row) for 2003–2016. (c) Pixel-by-pixel correlations between seasonal total rainfall and  $\Delta TWS$  for MAM and OND (stippling applied where correlations fall below the 95% significance level). (d) Same as (c) but with seasonal rainfall above the 95th percentile rather than total rainfall. In panels (a and b), the MAM years with the strongest zonal Pacific gradient are outlined with a red border and OND years with the strongest positive IOD years are outlined with a blue border.

in the >95th percentile contributes to >10 fold of the variance than the  $\leq 95$ th percentile across most of HAD during OND, and across central Kenya and the Kenya–Somalia borderland during MAM (Figure S9 in Supporting Information S1).

In general, GRACE TWS represents all surface water, SM in shallow layers, deep SM, and groundwater (e.g., Wahr et al., 2004). Since the HAD region (east of the African Great Lakes) largely lacks surface water because of its semi-arid/arid climate (Figure S5 in Supporting Information S1), that leaves SM, deep SM, and groundwater in the TWS signal. We find that  $\Delta SM$  values across HAD are at least an order of magnitude smaller than  $\Delta TWS$  values for both rainy seasons (Figure S11a in Supporting Information S1), and that the correlation between seasonal rainfall and  $\Delta SM$  is spatially restricted for both seasons (Figure S11b in Supporting Information S1). Finally, we find zero or negative trends in SM across the HAD region (Figure S11c in Supporting Information S1). Taken together, these results lead us to conclude that SM comprises a very small part (if any) of the TWS signal across HAD, strongly suggesting that annual and seasonal TWS trends are dominated by water storage changes in deeper soil layers (below 10 cm) and in groundwater aquifers. Figure 4 summarizes all our trend results for the

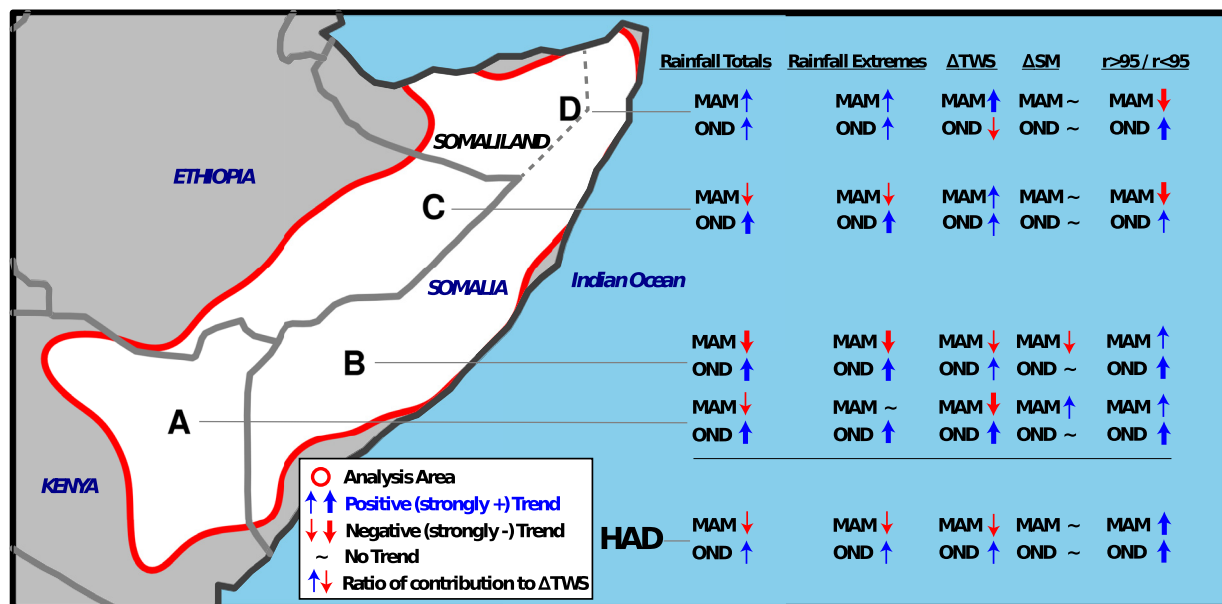


**Figure 4.** Trends in rainfall, total water storage (TWS), soil moisture (SM), and extreme contributions to TWS. Direction of trends in total and extreme rainfall between 1981 and 2019, TWS and SM between 2003 and 2016 at four roughly equidistant locations in Horn of Africa Dryland (HAD; Figure 2a) and averaged over the entire HAD. Trends are shown where the linear slope on the trend exceeds 0.1 mm/yr. Also shown is the ratio of variance in  $\Delta TWS$  explained by extreme ( $r > 95$ ) versus non-extreme rainfall ( $r < 95$ ) from Figure S9 in Supporting Information S1, where red arrows indicate ratios  $< 1$ , blue arrows show ratios  $> 1$ , and thick blue arrows indicate ratios  $> 2$  and thick red arrows ratios  $< 0.5$ . Trend values and correlation coefficients of the variables with time are listed in Table S2 in Supporting Information S1. National boundaries are shown in gray, and the political boundary of Somaliland as a gray dashed line.

various parts of HAD and averaged for the HAD as a whole, in terms of total seasonal rainfall, extreme seasonal rainfall, TWS, SM, and the contributions to  $\Delta TWS$  from the ratio of extreme ( $r > 95$ ) to non-extreme ( $r < 95$ ) rainfall, where arrows represent the direction of trends and thickness indicates trend strength.

#### 4. Discussion

In this paper, we investigated trends in seasonal rainfall within the HAD and their potential impact on regional water storage. The six rainfall data sets analyzed here corroborate previously documented seasonal rainfall trends in HAD for recent decades, showing that MAM rains have declined (Funk et al., 2005, 2008; Liebmann et al., 2014; Lyon & DeWitt, 2012; Williams & Funk, 2011). This multi-decadal decline is most strongly expressed in the latter part of the MAM rainy season, suggesting a possible shift in rainfall timing and/or a weakening of the climate drivers of rainfall in this season (Liebmann et al., 2014; Nicholson, 2017; Wainwright et al., 2019). Our analysis also showed a stronger and positive trend in OND rainfall, wherein seasonal totals have increased by 0.5–1.0 mm/yr in both October and November (Figure 1a), punctuated by positive IOD events that contributed to recent large regional floods and are projected to occur more frequently in the future (FEWSNET Special Report, 2020; Funk et al., 2018). Furthermore, we found that TWS has increased across HAD, in agreement with a recent analysis of trends in the Ogaden-Juba aquifer (Scanlon et al., 2022).

Over the past 20 years, there have been ocean-atmosphere teleconnections affecting the HAD rainfall (Funk et al., 2014; Liebmann et al., 2014). These include a zonal SST gradient in the Pacific, associated with low rainfall (drought) in MAM (Funk, Pedreros, et al., 2019; Funk et al., 2018) and a clear link between the IOD and high OND rainfall (MacLeod et al., 2020; Nicholson, 2017). Our research bears out these phenomena and their potential impacts on water resources across the HAD. We identify a link between positive IOD years (2006, 2011, and 2015), high OND rainfall, and large positive  $\Delta TWS$  (Figures 3a and 3b), as well as particular years of low MAM rainfall associated with the zonal SST gradient in the Pacific (2008, 2011, and 2012; Funk et al., 2018), leading to small and/or negative  $\Delta TWS$  (Figures 3a and 3b).

Since high intensity rainfall is a demonstrated driver of groundwater recharge in East African drylands (Cuthbert et al., 2019; Taylor et al., 2013; Thompson et al., 2019), the large (MAM) and rising (OND) rainfall extremes are

likely to be driving the correlation between seasonal rainfall extremes and  $\Delta$ TWS. In other words, any recharge of deep SM and groundwater from one dry season to the next is likely controlled by the most intense rainstorms of the intermediate rainy period, forcing deep local infiltration across the landscape (diffuse recharge) and producing runoff that becomes streamflow in channels. This streamflow subsequently infiltrates through porous channel beds (focused recharge) that are typical of dryland regions, thus supporting regional groundwater aquifers (Cuthbert et al., 2019; Jaeger et al., 2017; Singer & Michaelides, 2017). Recent research highlighted the renewability of groundwater storage across much of Africa (MacAllister et al., 2020; McDonald, 2021), but it lacked in situ groundwater data for HAD, one of the most food- and water-insecure and data-sparse regions in Africa. Our findings support the mechanism of deep-water recharge by extreme rainfall across HAD, contributing to a water store that persists and accumulates over decades, despite frequent droughts.

An important question is how seasonal rainfall in HAD will evolve in the future and what impacts it will have on water storage. Although CMIP3 and CMIP5 climate model simulations consistently project increased rainfall in both rainy seasons (e.g., Ongoma et al., 2018), the “East Africa Climate Paradox” highlights major concerns within the climate community about the veracity of these increasing projections, particularly for MAM in the face of observed negative rainfall trends from gridded data (Nicholson, 2017; Wainwright et al., 2019). These model projections for a wetter MAM may be in part based on theoretical increases in rainfall intensity for HAD, due to atmospheric warming via the Clausius-Clapeyron relation, leading to rainfall delivery in fewer, but more intense events (Chadwick et al., 2015; Trenberth, 2011). However, the magnitude of the MAM rainfall changes and the responsible dynamics within the models are unclear (Rowell, 2019; Shongwe et al., 2011). For OND, strong ENSO (Cai, Borlace, et al., 2014) and IOD events (Cai, Santoso, et al., 2014; Tierney et al., 2015) are projected to increase under anthropogenic climate change promoting more intense rainfall. Although higher intensity rainfall is associated with increased flood risk, the silver lining is that the increased channel runoff (floods) leads to higher rates of focused groundwater recharge with potential benefits for water security across the HAD region (Figures 3 and 4).

## 5. Conclusions

Our analysis of rainfall and water storage data sets showed that while total seasonal rainfall has declined in HAD over recent decades, especially during the agriculturally important MAM rainy season, TWS increased over the period 2003–2016. Furthermore, we showed that seasonal TWS dynamics are correlated with rainfall anomalies, and that positive trends in rainfall above the 95th intensity percentile is the major signal in this correlation. The ongoing trend of increasing water storage across HAD is potentially significant for drought adaptation and sustainability of water resources in this region. Economic and food security of HAD households are tightly linked to agricultural and pastoral livelihoods that depend on water availability under a changing climate. As of July 2022, drought-related food insecurity in Kenya and Somalia has pushed 18.6–21.1 million people into extreme (pre-famine) food insecurity (FSNWG Drought Special Report July, 2022). Hence, the link between increasing groundwater and rainfall extremes, described here for the HAD, may provide a valuable path towards regional climate adaptation and disaster risk reduction (United Nations, 2011). For example, a recent case study from Ethiopian drylands showed that groundwater may be a feasible water source for irrigation (Gowing et al., 2020). Given the dependence of rainfed agriculture on seasonal rains, which have repeatedly failed in recent decades, higher availability of groundwater for irrigated agriculture could potentially buffer the negative impacts of drought. The potential usefulness of groundwater depends on sufficient awareness of this water storage, its quality, accessibility as well as investment into relevant infrastructure to exploit it. In 2019/2020 this region experienced extreme precipitation, which was then followed by poor OND/MAM 2020/21, OND/MAM 2021/2022 rainy seasons, and as we write, a multi-year La Nina threatens to bring low rains again in OND 2022. It is possible that the stored water from the 2019/2020 rains could provide water resources to help buffer these more recent deficits.

Our analysis also suggests that it may be straightforward to identify parts of HAD where groundwater will become more abundant in the future, especially since the larger inter-annual variability implies that multi-year droughts are less likely for both rainy seasons in a row (Funk et al., 2018). Such an analysis, along with investment in an observational network of high-resolution rain gauges, SM sensors, and groundwater monitoring wells, could be used to identify cost-effective investment in local sand dams and even groundwater pumping equipment for broad regional benefit (MacDonald et al., 2009). Our findings suggest that groundwater in HAD is sustainable under the



prevailing climate, and that rural subsistence communities of the HAD may have an opportunity to become more resilient to climatic shocks in the future based on increasing and sustainable groundwater reserves.

### Conflict of Interest

The authors declare no conflicts of interest relevant to this study.

### Data Availability Statement

All data we used is publicly available from the respective data archives (see also Table S1 in Supporting Information S1 for data set-specific information). Total water storage data was obtained from [http://earth2observe.eu/files/Public%20Deliverables/D5.1\\_Report%20on%20the%20WRR1%20tier1.pdf](http://earth2observe.eu/files/Public%20Deliverables/D5.1_Report%20on%20the%20WRR1%20tier1.pdf) and <http://www2.csr.utexas.edu/grace/RL06.html>. Rainfall data was obtained from repositories outlined in Funk et al. (2015, <https://data.chc.ucsb.edu/products/CHIRPS-2.0/>), Beck et al. (2019, <http://www.gloh2o.org/mswep>), Harris and Jones (2017, [http://data.ceda.ac.uk/badc/cru/data/cru\\_ts/cru\\_ts\\_4.01](http://data.ceda.ac.uk/badc/cru/data/cru_ts/cru_ts_4.01)), Schneider et al. (2014, <https://www.esrl.noaa.gov/psd/data/gridded/data.gpcc.html>), Novella and Thiaw (2013, <http://iridl.ldeo.columbia.edu/SOURCES/.NOAA/.NCEP/.CPC/.FEWS/.Africa/.DAILY/.ARC2/.daily>), and Copernicus Climate Change Service (C3S) (2017, <https://doi.org/10.24381/cds.e2161bac>). The custom code to repeat our analysis and reproduce the figures can be obtained from <https://doi.org/10.5281/zenodo.5554732>.

### Acknowledgments

This research utilized computing facilities of the Bristol Research Initiative for the Dynamic Global Environment (BRIDGE). M.A. thanks Peter Peterson and Diego Pedreros for their support with CHIRPS analysis. The authors acknowledge funding from the following sources: the Global Challenges Research Fund (GCRF) (“Drought Risk in East African Drylands-DREAD” and “Impacts of Climate Change on the Water Balance in East African Drylands”); The Royal Society (“DRIER,” CHL/R1/180485); the European Union’s Horizon 2020 Program (“DOWN2EARTH,” 869550); the Natural Environment Research Council (NE/N014057/1); the USGS Drivers of Drought Program; the USAID Famine Early Warnings Systems Network; and the NASA’s Global Precipitation Measurement Mission (80NSSC19K0686).

### References

- Agutu, N. O., Awange, J. L., Zerihun, A., Ndehedehe, C. E., Kuhn, M., & Fukuda, Y. (2017). Assessing multi-satellite remote sensing, reanalysis, and land surface models' products in characterizing agricultural drought in East Africa. *Remote Sensing of Environment*, *194*, 287–302. <https://doi.org/10.1016/j.rse.2017.03.041>
- Amrhein, V., Greenland, S., & McShane, B. (2019). *Scientists rise up against statistical significance*. Nature Publishing Group.
- Apurv, T., Sivapalan, M., & Cai, X. (2017). Understanding the role of climate characteristics in drought propagation. *Water Resources Research*, *53*(11), 9304–9329. <https://doi.org/10.1002/2017wr021445>
- Beck, H. E., Wood, E. F., Pan, M., Fisher, C. K., Miralles, D. G., Van Dijk, A. I., et al. (2019). MSWEP V2 global 3-hourly 0.1 precipitation: Methodology and quantitative assessment. *Bulletin of the American Meteorological Society*, *100*(3), 473–500. <https://doi.org/10.1175/bams-d-17-0138.1>
- Bonsor, H. C., Shamsudduha, M., Marchant, B. P., MacDonald, A. M., & Taylor, R. G. (2018). Seasonal and decadal groundwater changes in African Sedimentary aquifers estimated using GRACE products and LSMs. *Remote Sensing*, *10*(6), 904. <https://doi.org/10.3390/rs10060904>
- Copernicus Climate Change Service (C3S). (2017). ERA5: Fifth generation of ECMWF atmospheric reanalyses of the global climate. *Copernicus Climate Change Service Climate Data Store (CDS)*, *15*(2), 2020.
- Cai, W., Borlace, S., Lengaigne, M., Van Rensch, P., Collins, M., Vecchi, G., et al. (2014). Increasing frequency of extreme El Niño events due to greenhouse warming. *Nature Climate Change*, *4*(2), 111–116. <https://doi.org/10.1038/nclimate2100>
- Cai, W., Santoso, A., Wang, G., Weller, E., Wu, L., Ashok, K., et al. (2014). Increased frequency of extreme Indian Ocean Dipole events due to greenhouse warming. *Nature*, *510*(7504), 254–258. <https://doi.org/10.1038/nature13327>
- Calow, R. C., MacDonald, A. M., Nicol, A. L., & Robins, N. S. (2010). Ground water security and drought in Africa: Linking availability, access, and demand. *Ground Water*, *48*(2), 246–256. <https://doi.org/10.1111/j.1745-6584.2009.00558.x>
- Chadwick, R., Good, P., Martin, G., & Rowell, D. P. (2015). Large rainfall changes consistently projected over substantial areas of tropical land. *Nature Climate Change*, *6*(2), 177–181. <https://doi.org/10.1038/nclimate2805>
- Cuthbert, M. O., Taylor, R. G., Favreau, G., Todd, M. C., Shamsudduha, M., Villholth, K. G., et al. (2019). Observed controls on resilience of groundwater to climate variability in sub-Saharan Africa. *Nature*, *572*(7768), 230–234. <https://doi.org/10.1038/s41586-019-1441-7>
- Dunning, C. M., Black, E., & Allan, R. P. (2018). Later wet seasons with more intense rainfall over Africa under future climate change. *Journal of Climate*, *31*(23), 9719–9738. <https://doi.org/10.1175/JCLI-D-18-0102.1>
- FAO, IFAD, UNICEF, WFP, & WHO. (2019). *The state of food security and nutrition in the world 2019. Safeguarding against economic slow-downs and downturns*. FAO.
- FEWSNET. (2021). East Africa Food Security Alert: Over 20 million people in need of urgent food aid in the Horn of Africa amid severe drought and conflict. Retrieved from [https://fewns.net/sites/default/files/documents/reports/east-africa-alert-20211229-final\\_0.pdf](https://fewns.net/sites/default/files/documents/reports/east-africa-alert-20211229-final_0.pdf)
- FEWSNET Special Report. (2020). 2019 Short rains in east Africa among the wettest on historical record. Retrieved from [https://fewns.net/sites/default/files/documents/reports/East\\_Africa\\_Special\\_Report\\_January\\_2020\\_Final\\_3.pdf](https://fewns.net/sites/default/files/documents/reports/East_Africa_Special_Report_January_2020_Final_3.pdf)
- Funk, C. (2012). Exceptional warming in the Western Pacific-Indian Ocean Warm Pool has contributed to more frequent droughts in Eastern Africa. *Bulletin of the American Meteorological Society*, *93*, 1049–1051.
- Funk, C., Dettinger, M. D., Michaelsen, J. C., Verdin, J. P., Brown, M. E., Barlow, M., & Hoell, A. (2008). Warming of the Indian Ocean threatens eastern and southern African food security but could be mitigated by agricultural development. *Proceedings of the National Academy of Sciences*, *105*(32), 11081–11086. <https://doi.org/10.1073/pnas.0708196105>
- Funk, C., Harrison, L., Shukla, S., Pomposi, C., Galu, G., Korecha, D., et al. (2018). Examining the role of unusually warm Indo-Pacific sea surface temperatures in recent African droughts. *Quarterly Journal of the Royal Meteorological Society*, *144*(S1), 360–383. <https://doi.org/10.1002/qj.3266>
- Funk, C., Hoell, A., Shukla, S., Bladé, I., Liebmann, B., Roberts, J. B., et al. (2014). Predicting East African spring droughts using Pacific and Indian Ocean sea surface temperature indices. *Hydrology and Earth System Sciences*, *18*(12), 4965–4978. <https://doi.org/10.5194/hess-18-4965-2014>

- Funk, C., Pedreros, D., Nicholson, S., Hoell, A., Korecha, D., Galu, G., et al. (2019). Examining the potential contributions of extreme 'Western V' sea surface temperatures to the 2017 March–June East African drought. *Bulletin of the American Meteorological Society*, *100*(1), S55–S60. <https://doi.org/10.1175/bams-d-18-0108.1>
- Funk, C., Peterson, P., Landsfeld, M., Pedreros, D., Verdin, J., Shukla, S., et al. (2015). The climate hazards infrared precipitation with stations—A new environmental record for monitoring extremes. *Scientific Data*, *2*(1), 150066. <https://doi.org/10.1038/sdata.2015.66>
- Funk, C., Senay, G., Asfaw, A., Verdin, J., Rowland, J., Korecha, D., et al. (2005). *Recent drought tendencies in Ethiopia and equatorial-subtropical eastern Africa*. FEWS-NET.
- Funk, C., Shukla, S., Thiaw, W. M., Rowland, J., Hoell, A., McNally, A., et al. (2019). Recognizing the famine early warning systems network: Over 30 years of drought early warning Science advances and partnerships promoting global food security. *Bulletin of the American Meteorological Society*, *100*(6), 1011–1027. <https://doi.org/10.1175/bams-d-17-0233.1>
- Funk, C., Thomas, P., Roy, V., & Way-Henthorne, J. (2019). Examining the Socioeconomic context of recent East African food insecurity. CHC Blog. Retrieved from <http://blog.chc.ucsb.edu/?p=634>
- FSNWG Drought Special Report July. (2022). Retrieved from <https://reliefweb.int/report/ethiopia/fsnwg-drought-special-report-july-2022>
- Gowing, J., Walker, D., Parkin, G., Forsythe, N., Haile, A. T., & Ayenew, D. A. (2020). Can shallow groundwater sustain small-scale irrigated agriculture in sub-Saharan Africa? Evidence from N-W Ethiopia. *Groundwater for Sustainable Development*, *10*, 100290. <https://doi.org/10.1016/j.gsd.2019.100290>
- Harris, I., & Jones, P. (2017). *CRU TS4. 01: Climatic Research Unit (CRU) Time-Series (TS) version 4.01 of high-resolution gridded data of month-by-month variation in climate (Jan. 1901–Dec. 2016)* (p. 25). Centre for Environmental Data Analysis.
- Harrison, L., Funk, C., & Peterson, P. (2019). Identifying changing precipitation extremes in Sub-Saharan Africa with gauge and satellite products. *Environmental Research Letters*, *14*(8), 085007. <https://doi.org/10.1088/1748-9326/ab2cae>
- Jaeger, K. L., Sutfin, N. A., Tooth, S., Michaelides, K., & Singer, M. (2017). Geomorphology and sediment regimes of intermittent rivers and ephemeral streams. In *Intermittent rivers and ephemeral streams* (pp. 21–49). Academic Press.
- Kipkemoi, I., Michaelides, K., Rosolem, R., & Singer, M. B. (2021). Climatic expression of rainfall on soil moisture dynamics in drylands. *Hydrology and Earth System Sciences Discussions*, *2021*, 1–24. <https://doi.org/10.5194/hess-2021-48>
- Kolusu, S. R., Shamsudduha, M., Todd, M. C., Taylor, R. G., Seddon, D., Kashaigili, J. J., et al. (2019). The El Niño event of 2015–2016: Climate anomalies and their impact on groundwater resources in east and southern Africa. *Hydrology and Earth System Sciences*, *23*(3), 1751–1762. <https://doi.org/10.5194/hess-23-1751-2019>
- Liebmann, B., Hoerling, M. P., Funk, C., Blade, I., Dole, R. M., Allured, D., et al. (2014). Understanding recent Eastern Horn of Africa rainfall variability and change. *Journal of Climate*, *27*(23), 8630–8645. <https://doi.org/10.1175/jcli-d-13-00714.1>
- Lorenz, C., & Kunstmann, H. (2012). The hydrological cycle in three state-of-the-art reanalyses: Intercomparison and performance analysis. *Journal of Hydrometeorology*, *13*(5), 1397–1420. <https://doi.org/10.1175/jhm-d-11-088.1>
- Lyon, B., & DeWitt, D. G. (2012). A recent and abrupt decline in the East African long rains. *Geophysical Research Letters*, *39*(2). <https://doi.org/10.1029/2011gl050337>
- MacAllister, D. J., MacDonald, A. M., Kebede, S., Godfrey, S., & Calow, R. (2020). Comparative performance of rural water supplies during drought. *Nature Communications*, *11*(1), 1–13. <https://doi.org/10.1038/s41467-020-14839-3>
- Macdonald, A. M., Calow, R. C., Macdonald, D. M. J., Darling, W. G., & Dochartaigh, B. É. Ó. (2009). What impact will climate change have on rural groundwater supplies in Africa? *Hydrological Sciences Journal*, *54*(4), 690–703. <https://doi.org/10.1623/hysj.54.4.690>
- MacLeod, D., Graham, R., O'Reilly, C., Otieno, G., & Todd, M. (2020). Causal pathways linking different flavours of ENSO with the Greater Horn of Africa short rains. *Atmospheric Science Letters*, *22*(2), e1015. <https://doi.org/10.1002/asl.1015>
- Maidment, R. I., Allan, R. P., & Black, E. (2015). Recent observed and simulated changes in precipitation over Africa. *Geophysical Research Letters*, *42*(19), 8155–8164. <https://doi.org/10.1002/2015gl065765>
- McDonald, J. P. (2021). Measuring a low horizontal hydraulic gradient in a high transmissivity aquifer. *Ground Water*, *59*(5), 694–709. <https://doi.org/10.1111/gwat.13091>
- Mileham, L., Taylor, R. G., Todd, M., Tindimugaya, C., & Thompson, J. (2009). The impact of climate change on groundwater recharge and runoff in a humid, equatorial catchment: Sensitivity of projections to rainfall intensity. *Hydrological Sciences Journal*, *54*(4), 727–738. <https://doi.org/10.1623/hysj.54.4.727>
- Nicholson, S. E. (2017). Climate and climatic variability of rainfall over eastern Africa. *Reviews of Geophysics*, *55*(3), 590–635. <https://doi.org/10.1002/2016RG000544>
- Novella, N. S., & Thiaw, W. M. (2013). African rainfall climatology version 2 for famine early warning systems. *Journal of Applied Meteorology and Climatology*, *52*(3), 588–606. <https://doi.org/10.1175/jamc-d-11-0238.1>
- Ongoma, V., Chen, H., & Gao, C. (2018). Projected changes in mean rainfall and temperature over East Africa based on CMIP5 models. *International Journal of Climatology*, *38*(3), 1375–1392. <https://doi.org/10.1002/joc.5252>
- Quichimbo, E. A., Singer, M. B., & Cuthbert, M. O. (2020). Characterising groundwater–surface water interactions in idealised ephemeral stream systems. *Hydrological Processes*, *34*(18), 3792–3806. <https://doi.org/10.1002/hyp.13847>
- Roca, R. (2019). Estimation of extreme daily precipitation thermodynamic scaling using gridded satellite precipitation products over tropical land. *Environmental Research Letters*, *14*(9), 095009. <https://doi.org/10.1088/1748-9326/ab35c6>
- Rowell, D. P. (2019). An observational constraint on CMIP5 projections of the East African long rains and southern Indian Ocean warming. *Geophysical Research Letters*, *46*(11), 6050–6058. <https://doi.org/10.1029/2019gl082847>
- Scanlon, B. R., Rateb, A., Anyamba, A., Kebede, S., MacDonald, A. M., Shamsudduha, M., et al. (2022). Linkages between GRACE water storage, hydrologic extremes, and climate teleconnections in major African aquifers. *Environmental Research Letters*, *17*(1), 014046. <https://doi.org/10.1088/1748-9326/ac3bfc>
- Schneider, U., Becker, A., Finger, P., Meyer-Christoffer, A., Ziese, M., & Rudolf, B. (2014). GPCP's new land surface precipitation climatology based on quality-controlled in situ data and its role in quantifying the global water cycle. *Theoretical and Applied Climatology*, *115*(1–2), 15–40. <https://doi.org/10.1007/s00704-013-0860-x>
- Shamsudduha, M., & Taylor, R. G. (2020). Groundwater storage dynamics in the world's large aquifer systems from GRACE: Uncertainty and role of extreme precipitation. *Earth System Dynamics*, *11*(3), 755–774. <https://doi.org/10.5194/esd-11-755-2020>
- Shongwe, M. E., van Oldenborgh, G. J., van den Hurk, B., & van Aalst, M. (2011). Projected changes in mean and extreme precipitation in Africa under global warming. Part II: East Africa. *Journal of Climate*, *24*(14), 3718–3733. <https://doi.org/10.1175/2010JCLI2883.1>
- Singer, M. B., & Michaelides, K. (2017). Deciphering the expression of climate change within the Lower Colorado River basin by stochastic simulation of convective rainfall. *Environmental Research Letters*, *12*(10), 104011. <https://doi.org/10.1088/1748-9326/aa8e50>
- Taylor, R. G., Todd, M. C., Kongola, L., Maurice, L., Nahozya, E., Sanga, H., & MacDonald, A. M. (2013). Evidence of the dependence of groundwater resources on extreme rainfall in East Africa. *Nature Climate Change*, *3*(4), 374–378. <https://doi.org/10.1038/nclimate1731>

- Thomson, P., Bradley, D., Katilu, A., Katuva, J., Lanzoni, M., Koehler, J., & Hope, R. (2019). Rainfall and groundwater use in rural Kenya. *Science of the Total Environment*, 649, 722–730. <https://doi.org/10.1016/j.scitotenv.2018.08.330>
- Tierney, J. E., Ummenhofer, C. C., & DeMenocal, P. B. (2015). Past and future rainfall in the Horn of Africa. *Science Advances*, 1(9), e1500682. <https://doi.org/10.1126/sciadv.1500682>
- Trenberth, K. (2011). Changes in precipitation with climate change. *Climate Research*, 47(1), 123–138. <https://doi.org/10.3354/cr00953>
- United Nations. (2011). Global drylands: A UN system-wide response (Tech. Rep.). Retrieved from [https://www.unep-wcmc.org/system/data-set\\_file\\_fields/files/000/000/091/original/Global-Drylands-FINAL-LR.pdf?1398440625](https://www.unep-wcmc.org/system/data-set_file_fields/files/000/000/091/original/Global-Drylands-FINAL-LR.pdf?1398440625)
- Verdin, J., Funk, C., Senay, G., & Choullarton, R. (2005). Climate Science and famine early warning. *Philosophical Transactions of the Royal Society B: Biological Sciences*, 360(1463), 2155–2168. <https://doi.org/10.1098/rstb.2005.1754>
- Wahr, J., Swenson, S., Zlotnicki, V., & Velicogna, I. (2004). Time-variable gravity from GRACE: First results. *Geophysical Research Letters*, 31(11), L11501. <https://doi.org/10.1029/2004gl019779>
- Wainwright, C. M., Marsham, J. H., Keane, R. J., Rowell, D. P., Finney, D. L., Black, E., & Allan, R. P. (2019). ‘Eastern African Paradox’ rainfall decline due to shorter not less intense Long Rains. *npj Climate and Atmospheric Science*, 2(1), 1–9. <https://doi.org/10.1038/s41612-019-0091-7>
- Williams, P., & Funk, C. (2011). A westward extension of the warm pool leads to a westward extension of the Walker circulation, drying eastern Africa. *Climate Dynamics*, 37, 2417–2435. <https://doi.org/10.1007/s00382-010-0984-y>

## References From the Supporting Information

- Allen, R. G., Pereira, L. S., Raes, D., & Smith, M. (1998). Crop evapotranspiration—Guidelines for computing crop water requirements. In *FAO irrigation and drainage paper 56* (pp. D05109). FAO.
- Beck, H. E., Van Dijk, A. I., Levizzani, V., Schellekens, J., Gonzalez Miralles, D., Martens, B., & De Roo, A. (2017). MSWEP: 3-hourly 0.25 global gridded precipitation (1979–2015) by merging gauge, satellite, and reanalysis data. *Hydrology and Earth System Sciences*, 21(1), 589–615. <https://doi.org/10.5194/hess-21-589-2017>
- Benjamini, Y., & Hochberg, Y. (1995). Controlling the false discovery rate: A practical and powerful approach to multiple testing. *Journal of the Royal Statistical Society: Series B*, 57(1), 289–300. <https://doi.org/10.1111/j.2517-6161.1995.tb02031.x>
- Chen, J., Famiglietti, J. S., Scanlon, B. R., & Rodell, M. (2016). Groundwater storage changes: Present status from GRACE observations. In *Remote sensing and water resources* (pp. 207–227). Springer.
- Chen, J. L., Wilson, C. R., Famiglietti, J. S., & Rodell, M. (2007). Attenuation effect on seasonal basin-scale water storage changes from GRACE time-variable gravity. *Journal of Geodesy*, 81(4), 237–245. <https://doi.org/10.1007/s00190-006-0104-2>
- Dinku, T., Funk, C., Peterson, P., Maidment, R., Tadesse, T., Gadain, H., & Ceccato, P. (2018). Validation of the CHIRPS satellite rainfall estimates over eastern Africa. *Quarterly Journal of the Royal Meteorological Society*, 144(S1), 292–312. <https://doi.org/10.1002/qj.3244>
- Ferreira, V. G., Yong, B., Seitz, K., Heck, B., & Grombein, T. (2020). Introducing an improved GRACE global point-mass Solution—A case study in Antarctica. *Remote Sensing*, 12(19), 3197. <https://doi.org/10.3390/rs12193197>
- Forootan, E., Didova, O., Kusche, J., & Löcher, A. (2013). Comparisons of atmospheric data and reduction methods for the analysis of satellite gravimetry observations. *Journal of Geophysical Research: Solid Earth*, 118(5), 2382–2396. <https://doi.org/10.1002/jgrb.50160>
- Funk, C., Nicholson, S. E., Landsfeld, M., Klotter, D., Peterson, P., & Harrison, L. (2015). The centennial trends Greater Horn of Africa precipitation dataset. *Scientific Data*, 2(1), 1–17. <https://doi.org/10.1038/sdata.2015.50>
- Gilbert, R. O. (1987). *Statistical methods for environmental pollution monitoring*. John Wiley & Sons.
- IPCC AR5. (2015). The physical science basis. Working group I contribution to the fifth assessment report of the intergovernmental panel on climate change. Retrieved from <http://www.ipcc.ch/report/ar5/wg1>
- Kusche, J., Schmidt, R., Petrovic, S., & Rietbroek, R. (2009). Decorrelated GRACE time-variable gravity solutions by GFZ, and their validation using a hydrological model. *Journal of Geodesy*, 83(10), 903–913. <https://doi.org/10.1007/s00190-009-0308-3>
- Landerer, F. W., & Swenson, S. C. (2012). Accuracy of scaled GRACE terrestrial water storage estimates. *Water Resources Research*, 48(4), W04531. <https://doi.org/10.1029/2011wr011453>
- Mehrnagar, N., Jones, O., Singer, M. B., Schumacher, M., Bates, P., & Forootan, E. (2020). Comparing global hydrological models and combining them with GRACE by dynamic model data averaging (DMDA). *Advances in Water Resources*, 138, 103528. <https://doi.org/10.1016/j.advwatres.2020.103528>
- Roca, R., Alexander, L. V., Potter, G., Bador, M., Jucá, R., Contractor, S., et al. (2019). FROGS: A daily 1°×1° gridded precipitation database of rain gauge, satellite and reanalysis products. *Earth System Science Data*, 11(3), 1017–1035. <https://doi.org/10.5194/essd-11-1017-2019>
- Save, H., Bettadpur, S., & Tapley, B. D. (2016). High-resolution CSR GRACE RL05 mascons. *Journal of Geophysical Research: Solid Earth*, 121(10), 7547–7569. <https://doi.org/10.1002/2016JB013007>
- Sen, P. K. (1968). Estimates of the regression coefficient based on Kendall's tau. *Journal of the American Statistical Association*, 63(324), 1379–1389. <https://doi.org/10.1080/01621459.1968.10480934>
- Singer, M. B., Asfaw, D. T., Rosolem, R., Cuthbert, M. O., Miralles, D. G., MacLeod, D., et al. (2021). Hourly potential evapotranspiration at 0.1° resolution for the global land surface from 1981-present. *Scientific Data*, 8(1), 1–13. <https://doi.org/10.1038/s41597-021-01003-9>
- Swenson, S., Chambers, D., & Wahr, J. (2008). Estimating geocenter variations from a combination of GRACE and ocean model output. *Journal of Geophysical Research*, 113(B8), B08410. <https://doi.org/10.1029/2007jb005338>
- Theil, H. (1950). A rank-invariant method of linear and polynomial regression analysis, 3; confidence regions for the parameters of polynomial regression equations. *Indagationes Mathematicae*, 1(2), 467–482.
- Van Dijk, A. I. J. M., Renzullo, L. J., & Rodell, M. (2011). Use of Gravity Recovery and Climate Experiment terrestrial water storage retrievals to evaluate model estimates by the Australian water resources assessment system. *Water Resources Research*, 47(11), W11524. <https://doi.org/10.1029/2011wr010714>
- Ventura, V., Paciorek, C. J., & Risbey, J. S. (2004). Controlling the proportion of falsely rejected hypotheses when conducting multiple tests with climatological data. *Journal of Climate*, 17(22), 4343–4356. <https://doi.org/10.1175/3199.1>
- Wada, Y., Wisser, D., & Bierkens, M. F. (2014). Global modeling of withdrawal, allocation and consumptive use of surface water and groundwater resources. *Earth System Dynamics*, 5(1), 15–40. <https://doi.org/10.5194/esd-5-15-2014>
- Wang, H., Wu, P., & Wang, Z. (2006). An approach for spherical harmonic analysis of non smooth data. *Computers & Geosciences*, 32(10), 1654–1668. <https://doi.org/10.1016/j.cageo.2006.03.004>

- Watkins, M. M., Wiese, D. N., Yuan, D. N., Boening, C., & Landerer, F. W. (2015). Improved methods for observing Earth's time variable mass distribution with GRACE using spherical cap mascons. *Journal of Geophysical Research: Solid Earth*, *120*(4), 2648–2671. <https://doi.org/10.1002/2014jb011547>
- Wilks, D. (2016). “The stippling shows statistically significant grid points”: How research results are routinely overstated and overinterpreted, and what to do about it. *Bulletin of the American Meteorological Society*, *97*(12), 2263–2273. <https://doi.org/10.1175/bams-d-15-00267.1>